Momentum, motion and transport in fluids

Derive a flow from its conservation laws and boundary conditions. Quantify how length scales and material properties decide which approximation can predict a measurement.

Contents

1. **Gravity, capillarity and instability at a moving interface**
   A flat interface can carry waves restored by gravity and surface tension. If its two liquids or gases move at different speeds, a band of those waves can grow. Derive the ideal threshold, identify the most vulnerable wavelength at onset and distinguish growth of an instability from advection of an otherwise stable disturbance.
2. **Settling spheres, Stokes drag and a wall correction**
   A falling-sphere viscometer infers viscosity from terminal speed. Derive the drag on a no-slip sphere, distinguish creeping flow from merely steady motion and use radius, vessel width and orientation checks to decide what the speed experiment actually measures.
3. **Why shear disperses a tracer faster than molecular diffusion**
   A short dye pulse in a straight tube first stretches into a filament and much later resembles a broadened one-dimensional cloud. Derive the long-time Taylor–Aris coefficient, predict the width of a measured pulse and identify the mixing time needed before fitting the familiar one-dimensional approximation.
4. **Estimate wall drag by integrating a boundary-layer profile**
   A velocity probe can resolve the momentum missing from a boundary layer more easily than the wall shear itself. Derive an integral momentum relation, estimate drag using a polynomial profile and determine when a pressure gradient or a measurement too far from the wall changes the answer.
5. **How long does a moving wall take to set a fluid layer in motion?**
   Start the top of a narrow gap suddenly and follow the velocity, volume flow and wall stresses as viscous diffusion builds a Couette profile.
6. **How far upstream does a downstream water level matter?**
   A depth gauge downstream of a change in bed level measures a local state. Predict the depth one kilometre upstream by combining energy, cross-section geometry and a resistance law, then fit the roughness against independent uniform-flow readings.
7. **How can a constant-area duct choke?**

A nozzle reaches a sonic state by changing area. A straight pipe can approach the same Mach number through friction or through heating. The two cases conserve different combinations of stagnation properties.

Momentum, motion and transport in fluids · 1. Gravity, capillarity and instability at a moving interface

A flat interface can carry waves restored by gravity and surface tension. If its two liquids or gases move at different speeds, a band of those waves can grow. Derive the ideal threshold, identify the most vulnerable wavelength at onset and distinguish growth of an instability from advection of an otherwise stable disturbance.

Impose kinematic conditions on both fluids

Consider two immiscible inviscid incompressible fluids of effectively infinite depth. The lower fluid has density $\rho_1 > \rho_2$; base velocities U_1, U_2 are uniform and parallel to a horizontal interface at $z = 0$. Let its small displacement be $\eta e^{i(kx-\omega t)}$ with $k > 0$. Assume irrotational disturbances within each layer, so their potentials satisfy Laplace's equation. Decay away from the interface gives forms $A_1 e^{kz}$ below and $A_2 e^{-kz}$ above. An interfacial vortex sheet is still allowed because tangential base velocities differ.

A material point on either side stays on the perturbed interface in the normal direction. Applying $(\partial_t + U_j \partial_x)\eta = \partial_z \phi_j$ gives

$$A_1 = -i(\omega - kU_1)\eta/k,$$
$$A_2 = +i(\omega - kU_2)\eta/k.$$

Pressure perturbations from linear Bernoulli include both the unsteady potential and hydrostatic change at the displaced surface. Equating pressure jump to the surface-tension curvature force yields

$$\rho_1(\omega - kU_1)^2 + \rho_2(\omega - kU_2)^2 = (\rho_1 - \rho_2)gk + \sigma k^3.$$

Gravity restores long waves for the stated stable density ordering, while surface tension restores short waves. Check the equal-velocity limit: adding the same velocity to both layers merely Doppler-shifts the wave frequency and cannot make a stable interface unstable.

Complete the square and locate the first unstable wavelength

Define density-weighted velocity $\bar{U} = (\rho_1 U_1 + \rho_2 U_2)/(\rho_1 + \rho_2)$. The squared frequency relative to $k\bar{U}$ becomes the restoring right-hand side divided by total density minus $\rho_1\rho_2 k^2 (U_1 - U_2)^2/(\rho_1 + \rho_2)^2$. A negative value gives one exponentially growing and one decaying branch. In that regime the real frequency still advects with $k\bar{U}$, while growth rate is the square root of the negative discriminant's magnitude. A moving pattern alone is insufficient evidence of instability.

For each k, the squared critical relative speed is proportional to $(\rho_1 - \rho_2)g/k + \sigma k$. Differentiating gives the minimum at $k_* = \sqrt{(\rho_1 - \rho_2)g/\sigma}$. For densities 1000 and 1.2 kg/m³ and tension 0.072 N/m the onset wavelength is 17.0 mm, with ideal threshold 6.66 m/s. At 7.0 m/s the growth rate at this same wavelength is about 27.6 per second, an e-fold interval of 36 ms. The wavelength giving maximum growth above threshold can differ from the onset wavelength.

Open the live experiment

Try the calculation

Relative flow speed (m/s) 7

Surface tension (mN/m) 72

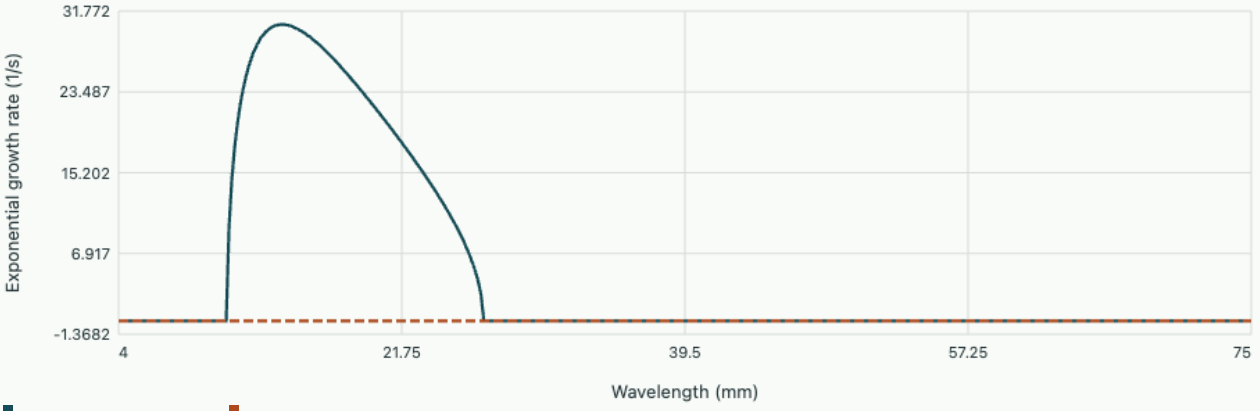

Selected flow At 90% of selected speed

The ideal minimum threshold is 6.66 m/s at wavelength 17.03 mm. At that wavelength selected growth is 27.6 per second.

Make a quantitative observation under controlled assumptions

A suitable numerical experiment starts from the same small disturbance amplitude for a set of Fourier modes and compares early exponential growth with the dispersion relation. If an initial ripple amplitude doubles from 0.10 to 0.20 mm in 25 ms, its estimated growth is $\log 2/0.025 = 27.7$ per second. Measure several early time windows and ensure amplitude remains small compared with wavelength. Nonlinear saturation, finite channel depth, viscosity, actual shear-layer thickness and wave generation at an inlet all change the late or measured growth. The ideal air–water threshold is not a prediction for wind-wave onset with an arbitrary atmospheric velocity profile.

Distinguish a convected disturbance from growth at one place

An unstable wave in the temporal calculation has a real wavelength and a complex frequency. Its visible crests are carried along by the density-weighted mean flow while its envelope grows. A fixed camera viewing a short section may see a larger wave on one side than on the other without observing a temporal increase at a fixed material phase. An inlet wavemaker, reflection, a varying channel depth and convective transport can each change the spatial pattern. Follow the same crest group with a time-stamped image sequence and inspect its early amplitude before the interface becomes strongly distorted.

As a simple measurement example, suppose a tracked narrow band grows from 0.20 mm to 0.40 mm in 0.10 seconds. The inferred temporal exponent is the natural logarithm of two divided by the elapsed time, or 6.93 per second. If noise adds a constant apparent amplitude floor, fitting logarithms of the

earliest images can suppress the inferred slope. Measure a quiet reference sequence and repeat the estimate over several windows. Once the slope falls substantially as amplitude increases, nonlinear saturation may have begun. Extrapolating the early exponential through the late stage then overestimates growth.

At the theoretical onset the predicted growth rate vanishes. This is the least convenient location for a finite observation interval because a weakly unstable wave may scarcely grow before it leaves the field of view. Compare a sequence of speeds on both sides of threshold and plot the squared measured growth rate against squared relative velocity at one chosen wavelength. The ideal dispersion relation gives a locally linear relation and suggests a more stable intercept estimate than judging the first visibly wavy frame.

Tutorial · Recover surface tension from the onset wavelength

At the same densities, an ideal calculation with a different liquid predicts the minimum threshold at wavelength 12.0 mm. Estimate surface tension. What independent measurement checks the model without reusing the wavelength?

▼ **Invert the onset condition**

With $k_* = 2\pi/0.012 = 524$ per metre, $\sigma = (998.8)(9.81)/k_*^2 = 0.0357$ N/m. Insert that value into the threshold-speed equation and compare with a measured critical relative velocity. Wavelength alone fixes the ratio of buoyancy and tension terms in this model; matching a second independent onset observable is a stronger test. Verify that the observed wavelength corresponds to first onset rather than the fastest mode at a substantially larger speed.

Tutorial · Distinguish finite growth from a short observation

A mode has predicted growth 5.0 per second but is visible in a camera field for only 30 ms as it advects. Estimate its amplitude increase. Could an apparently constant amplitude establish stability?

▼ **Compare residence and growth times**

The predicted factor is $e^{5(0.03)} = 1.162$, just sixteen percent. If amplitude noise, illumination variation or uncertainty in initial conditions is comparable, such a record cannot distinguish weak growth from neutral propagation. Measure along the convecting packet or extend the observable path, then fit log amplitude with calibrated spatial gain. A lack of measurable growth over one short camera region places only an upper bound on its rate.

Tutorial · Suppress tension in the mathematical model

Set surface tension to zero while retaining a sharp velocity discontinuity and stable gravity. What happens to the high-wavenumber threshold and why would finite-mesh simulations disagree as they are refined?

▼ **Examine the highest resolved modes**

The required squared speed then falls as $1/k$, so any nonzero velocity jump can destabilise sufficiently short waves. In the vortex-sheet idealisation their high-k growth rate scales with k. Refining a numerical mesh allows faster modes previously excluded by the grid. A physically smooth shear layer, surface tension, viscosity or other physical regularisation must be specified if the small-scale evolution is important. Numerical smoothing can control a calculation but its length scale is then part of the assumed model, not a measured material parameter.

MIT Interfacial Phenomena · surface waves and Kelvin–Helmholtz instability

Momentum, motion and transport in fluids · 2. Settling spheres, Stokes drag and a wall correction

A falling-sphere viscometer infers viscosity from terminal speed. Derive the drag on a no-slip sphere, distinguish creeping flow from merely steady motion and use radius, vessel width and orientation checks to decide what the speed experiment actually measures.

Balance pressure and viscosity around a sphere

Let a rigid sphere of radius a move with small relative speed U in a Newtonian fluid. In the sphere frame impose a uniform far flow $U\mathbf{e}_z$, no slip at its surface and incompressibility. If particle Reynolds number $\rho U(2a)/\mu$ is small, drop convective inertia, obtaining $-\nabla p+\mu\nabla^2\mathbf{u}=0$. Dimensional reasoning predicts a drag proportional to $\mu a U$ but cannot determine its prefactor. That prefactor depends on the no-slip surface and three-dimensional geometry.

The axisymmetric Stokes solution has $u_r=U\cos\theta[1-3a/(2r)+a^3/(2r^3)]$,

$$u_\theta=-U\sin\theta[1-3a/(4r)-a^3/(4r^3)],$$

$$p-p_\infty=-3\mu U a\cos\theta/(2r^2).$$

Substitution verifies zero surface velocity and the uniform far limit. The pressure contribution in the streamwise direction integrates as the surface integral of $-(p-p_\infty)\cos\theta$, giving $2\pi\mu a U$. Tangential viscous traction supplies $4\pi\mu a U$. Their sum gives

$$F_D=6\pi\mu a U,$$

$$C_D=\frac{24}{Re_D},$$

$$Re_D=\frac{2\rho a U}{\mu}.$$

A seemingly simpler potential-flow solution satisfying only impermeability misses the viscous traction and cannot reproduce the drag. Conversely a calculation that integrates just wall shear misses one third of this drag even at negligible inertia. The signs depend on whether one computes force of fluid on sphere or sphere on fluid; the magnitude above resists relative motion.

Balance buoyancy and find the terminal motion scale

A sphere of density $\rho_s>\rho$ has buoyancy-corrected weight $(4\pi a^3/3)(\rho_s-\rho)g$. Equating drag and this weight yields

$$U_t=2a^2(\rho_s-\rho)g/(9\mu).$$

Take $a=0.50$ mm, density difference 1200 kg/m³ and viscosity 0.50 Pa s. The unbounded terminal speed is 1.31 mm/s. For fluid density 1000 kg/m³, $Re_D=0.00262$, supporting a steady creeping-flow approximation. A 30 mm timed distance then takes about 22.9 s.

A coarse transient model uses sphere inertia alone, $m_s\dot{U} + 6\pi\mu a U = W_{\mathrm{eff}}$, predicting relaxation time $m_s/(6\pi\mu a)$. Actual transient hydrodynamics also contains added mass and a viscous-history contribution. Measuring a steady late portion is much safer than fitting the initial release with the simple exponential when extracting viscosity. Measure speed over successive equal intervals and check that it has become constant, away from both the release and vessel bottom.

Compare the viscous penetration time with the oscillating-wall experiment

A slow particle can still strongly interact with the container

A stationary no-slip cylindrical vessel increases drag on a sphere translating along its centreline. For small size ratio $\lambda = a/R_{\mathrm{tube}}$, the standard leading mobility correction is $U_{\mathrm{tube}}/U_{\infty} \simeq 1 - 2.1044\lambda + \cdots$. At $\lambda = 0.05$ the measured speed is already roughly ten percent smaller. Inserting that diminished speed into an unbounded drag law biases inferred viscosity upward. A small Reynolds number does not make walls irrelevant; it only addresses inertia relative to viscosity.

Measure terminal speed from a recorded trajectory

Choose a transparent column wide enough that the sphere remains many radii from its wall in the analysed window. Convert pixel distances to physical length using a scale in the same plane as the particle centre. Refraction through a curved vessel can otherwise give different apparent distances at the wall and centre. Fit position against time over several windows beginning after release. A stable slope with changing window length supports the terminal-speed interpretation; a trend in that slope can indicate acceleration, a fluid current or proximity to the bottom.

Open the live experiment

Try the calculation

Particle radius (µm)	10
Liquid viscosity (mPa s)	4
Density excess (kg/m³)	500

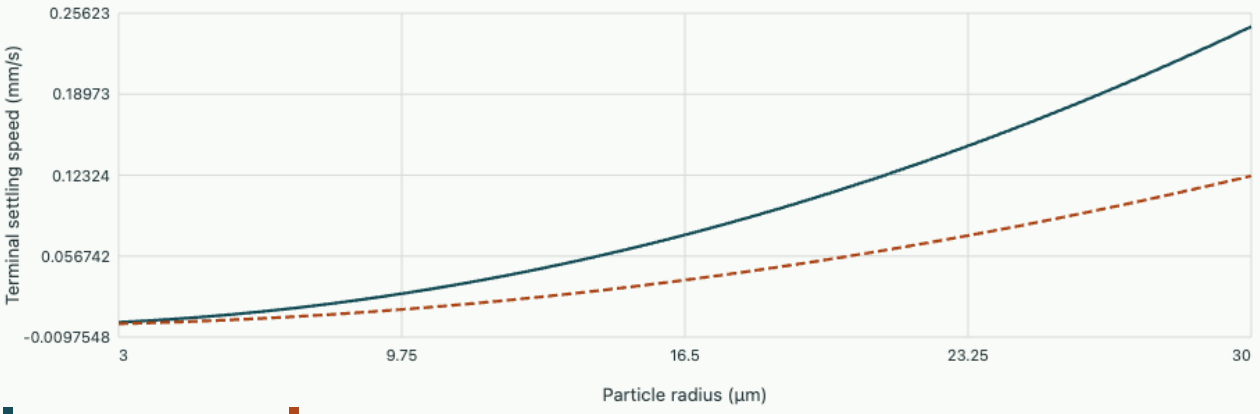

Selected viscosity Twice the viscosity

For the selected radius the Stokes prediction is 0.0272 mm/s, giving diameter Reynolds number 0.000136. Compare this number with unity before trusting the approximation.

The plot overlays the selected viscosity with a run at twice that viscosity. At fixed particle size their ideal terminal speeds differ by a factor of two. The horizontal axis invites a different comparison: the same settling speed in the more viscous fluid requires a radius larger by a factor of the square root of two. Use the numerical Reynolds number in the readout as a validity test. Increasing particle size tenfold raises terminal speed a hundredfold but diameter Reynolds number a thousandfold, so the apparent ease of tracking a larger particle has a fluid-mechanical cost.

A density inference can be especially fragile near neutral buoyancy. For example, if particle and liquid densities are 1020 and 1000 kilograms per cubic metre, an absolute uncertainty of two kilograms per cubic metre in each input is small relative to either density yet large relative to their difference. If independent it gives a standard uncertainty about 2.8 kilograms per cubic metre in the excess, or fourteen percent. Compare with the microscope radius calibration before attributing observed variation to the viscosity. Vertical temperature gradients can drive background circulation whose speed is comparable with a very slowly settling particle.

Tutorial · Estimate viscosity and its radius uncertainty

A sphere of radius 0.40 mm and density contrast 1000 kg/m³ falls at 0.80 mm/s far from walls. Infer viscosity and propagate an independent two-percent radius uncertainty, neglecting other errors.

▼ **Invert the terminal balance**

The inferred viscosity is $2(0.00040)^2(1000)(9.81)/[9(0.00080)] = 0.436$ Pa s. Its radius contribution to relative uncertainty is approximately four percent because radius is squared. If density contrast is estimated by subtracting two similar measured densities, its relative uncertainty can be much larger than either density's relative error. Repeat with a sufficiently well-characterised reference sphere and measure liquid temperature since viscosity can vary markedly with it.

Tutorial · Could a speed mismatch be wall drag?

For a 0.50 mm radius sphere and a 10 mm radius tube, the measured terminal speed is 1.17 mm/s rather than the 1.31 mm/s unbounded prediction. Check the leading wall correction and propose a test that does not assume the listed viscosity is exact.

▼ **Compare a vessel-size sequence**

The radius ratio is 0.050, so the leading correction predicts a factor 0.895 and speed 1.17 mm/s. Repeat in two or more wider tubes at unchanged temperature and fit speed against inverse tube radius. Extrapolation toward zero inverse radius estimates unbounded mobility without requiring the listed viscosity for the extrapolation. Off-axis migration, wall roughness, bottom confinement and finite-size higher terms must still be checked. One match to a leading coefficient does not prove perfect centring.

Tutorial · Brownian jitter or sustained background flow?

A much smaller tracer shows fluctuations in falling displacement and an unexpected common horizontal drift. How would you estimate its settling speed without attributing every displacement increment to gravity?

▼ **Separate first and second displacement moments**

Brownian motion adds variance increasing with lag in a diffusive interval but no mean drift in a homogeneous quiescent bath. Background flow adds a mean vector common to passive tracers. Measure many trajectories, estimate the fluid's mean velocity with a nearly neutrally buoyant marker and subtract it before fitting mean vertical drift. Fit the residual displacement variance separately to estimate diffusion and compare with the Einstein–Stokes prediction. A static temperature gradient can generate convection or thermophoresis, so repeat at several positions or orientations before assigning a gravity-only terminal balance.

MIT Advanced Environmental Fluid Mechanics · Stokes flow past a sphere

Momentum, motion and transport in fluids · 3. Why shear disperses a tracer faster than molecular diffusion

A short dye pulse in a straight tube first stretches into a filament and much later resembles a broadened one-dimensional cloud. Derive the long-time Taylor–Aris coefficient, predict the width of a measured pulse and identify the mixing time needed before fitting the familiar one-dimensional approximation.

Cross-sectional averaging leaves a correlated flux

Consider steady fully developed laminar Poiseuille flow of mean speed U in a circular tube of radius a. The axial profile is $u(r) = 2U(1 - r^2/a^2)$. A dilute passive solute of molecular diffusivity D is carried by this velocity and diffuses in all directions, with no solute flux at the wall. Section-averaging its advection–diffusion equation leaves a flux $\overline{uc}$. Splitting into mean and deviation gives $U\bar{c} + \overline{u'c'}$. It is the latter covariance that disperses the pulse beyond its molecular diffusion.

At times long compared with a transverse mixing scale of order a^2/D, and for a slowly varying axial average, take $c' \simeq f(r)\partial_z \bar{c}$. Substituting into the leading radial balance gives

$$D r^{-1}(r f')' = u - U = U(1 - 2r^2/a^2).$$

Regularity at the centre and zero wall derivative give

$$f' = (U/D)(r/2 - r^3/(2a^2)).$$

Integrate again and choose a constant so $\overline{f} = 0$. The section-integrated correlation is most easily evaluated by multiplying the radial equation by f and integrating by parts:

$$\overline{u'f} = -D\overline{(f')^2} = -\frac{U^2 a^2}{48 D},$$

$$D_{\mathrm{eff}} = D + \frac{U^2 a^2}{48 D}.$$

The negative sign means an average concentration gradient drives a net down-gradient dispersive flux. The molecular diffusivity in the denominator is not a paradox. Faster radial diffusion lets a tracer sample slow and fast streamlines more frequently and reduces long-time axial velocity memory. Taking D arbitrarily close to zero at a fixed observation time violates the long transverse-mixing requirement before the formula could diverge.

Predict a pulse width and its applicability window

For $a = 100$ micrometres, $U = 0.50$ mm/s and $D = 1.0 \times 10^{-9}$ square metres per second, $Ua/D = 50$ and $D_{\mathrm{eff}} = 5.31 \times 10^{-8}$ square metres per second. Radial mixing time a^2/D is about 10 s, corresponding to an advected length 5 mm. After 100 s, under long-tube and narrow-initial-pulse assumptions, the axial rms width is $\sqrt{2 D_{\mathrm{eff}} t} = 3.26$ mm while the mean pulse has travelled 50 mm. A velocity measured from width alone is ambiguous without an independent molecular diffusivity and a check of the time regime.

A detector at a fixed axial station records concentration versus time. Converting a small spatial width to a temporal width by division by U is a local approximation when the pulse is narrow compared with distance travelled and continues broadening slowly during its passage. An absorbing detector or outlet collecting solute flux can weight the distribution differently from a nonintrusive optical section-average. State whether the instrument measures local intensity, section-average concentration or total mass flux.

Recover the parabolic base profile in the viscous-duct chapter

Background · How does a finite injection pulse change the inferred dispersion?

A tracer valve introduces a plug of finite axial width. In the long-time regime with linear transport, the measured concentration is the convolution of the released profile with the spreading kernel. After normalising both to unit mass their variances add, just as variances add for independent displacements.

$$\sigma_x^2(t) = \sigma_{x,0}^2 + 2D_{\mathrm{eff}}t,$$

$$D_{\mathrm{eff}} = \frac{\sigma_x^2(t_2) - \sigma_x^2(t_1)}{2(t_2 - t_1)}.$$

A uniform 12 mm plug has initial variance $12^2/12 = 12$ mm². A one-time estimate forced through zero at $t = 10$ s therefore overestimates D_{eff} by 0.60 mm²/s. Two complete spatial images can eliminate the intercept if both are taken in the Taylor-dispersion regime. A camera that clips one tail does not record the full variance.

Read dispersion from the second moment of an image

After a short pulse has entered the straight observation tube, a camera integrates fluorescence across its diameter. Subtract a background frame and flat-field the illumination, integrate across the complete width, then compute the axial centroid and variance with concentration as weights. A constant gain cancels in both normalised moments. Saturating the brightest central pixels does not cancel: it reduces the measured peak more than the tails and biases the width. A window too narrow to capture the tails produces the opposite error. Shift and widen the analysis window as the pulse travels.

Open the live experiment

Try the calculation

Tube radius (µm) **100**

Mean velocity (mm/s) **0.5**

Molecular diffusivity (nm²/ns) **1**

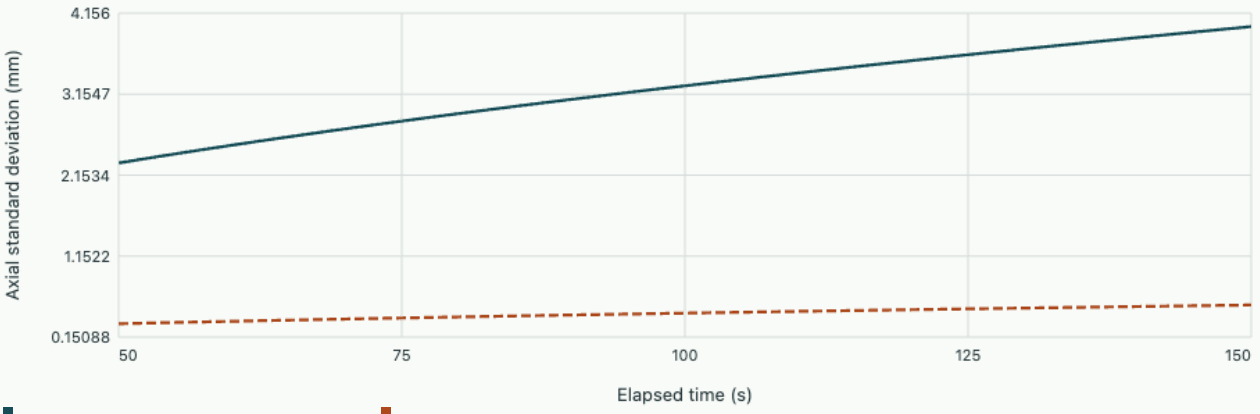

Radial mixing scale is 10.00 s and effective diffusivity is 5.308e-8 m²/s. Ten mixing times after injection the effective axial rms width is 3.26 mm.

The figure starts several radial mixing times after injection. Its left endpoint represents an already broadened pulse; the model was derived in this late regime. For an injection with appreciable initial variance, add that variance to the predicted diffusive growth instead of forcing the variance line through zero. With a constant axial imaging blur, variances likewise add under convolution with a normalised response. In that case two late measurements can identify a slope even if the intercept includes both injection width and camera blur. Recovering the initial width from the intercept would require an independent calibration.

The radius and velocity sliders are independent. To model a pump holding flow rate fixed when the radius is doubled, divide velocity by four as well. The effective enhancement then decreases by four and the radial mixing time increases by four. Comparing observations at the same absolute time could inadvertently move one case outside the long-time regime. Compare at a stated multiple of each radial mixing time and also record the corresponding distances needed along the tube.

Tutorial · Predict what a second pulse station should see

Two nonintrusive imaging stations observe the same well-mixed pulse after mean transit times 60 and 120 seconds under the example conditions. Estimate the increase in spatial variance. Why does differencing help with uncertainty in initial injection width?

▼ **Use the long-time variance slope**

The difference is $2D_{\mathrm{eff}}(120-60)=6.37\times10^{-6}$ square metres, or 6.37 square millimetres. An initial injection variance and any common Gaussian imaging blur add approximately constant offsets to the spatial variance and cancel in this difference. If the image point spread differs between stations or the first station is still within the shear-dominated entrance transient, cancellation fails. Check more than two stations to test linear variance growth before inferring a dispersion coefficient.

Tutorial · Compare a thinner tube at fixed volumetric rate

Halve the radius while keeping volumetric flow rate and molecular diffusivity fixed, assuming fully developed laminar flow remains valid. What happens to mean velocity, transverse mixing time, dispersive enhancement and required pressure gradient?

▼ **Keep the imposed quantity fixed**

Mean speed increases by four because area is quartered. Transverse mixing time falls by four. The enhancement $U^2a^2/(48D)$ increases by four. For Poiseuille flow at fixed volume rate the required axial pressure gradient scales as a^{-4}, hence increases by sixteen. At fixed mean velocity, in contrast, the enhancement would decrease by four. A claim that narrower tubes always improve or always suppress dispersion is incomplete without naming the operating constraint.

Tutorial · Interpret a non-Gaussian short-time profile

At a distance reached in only one second the optical image shows a long leading filament and a concentration tail near the wall. Does this invalidate the measured molecular diffusivity? Sketch the limiting motion if radial diffusion were absent during that interval.

▼ **Compare the observation time with the radial mixing time**

One second is only a tenth of the example transverse diffusion scale. Material near the centre moves near $2U$, while material close to a no-slip wall is almost stationary. An initially uniform cross-section pulse therefore separates by streamline velocity, covering a broad range of axial positions. A single effective Gaussian diffusion law has not yet emerged. Compare direct advection–diffusion with an independently measured initial profile, then check the long-time variance at larger distances. Wall adsorption would create additional lag even after radial mixing and can be tested by changing wall chemistry or solute type.

MIT Advanced Fluid Dynamics · section 4.7, dispersion and the Aris solution for a circular pipe

Momentum, motion and transport in fluids · 4. Estimate wall drag by integrating a boundary-layer profile

A velocity probe can resolve the momentum missing from a boundary layer more easily than the wall shear itself. Derive an integral momentum relation, estimate drag using a polynomial profile and determine when a pressure gradient or a measurement too far from the wall changes the answer.

Define displacement and momentum thickness separately

For steady incompressible two-dimensional flow over a smooth wall, let $U_e(x)$ denote the local speed just outside a thin attached boundary layer and $u(x,y)$ the tangential speed inside it. Displacement thickness $\delta^* = \int_0^\infty (1 - u/U_e)dy$ measures missing volume flow per unit outer speed. Momentum thickness $\theta = \int_0^\infty (u/U_e)(1 - u/U_e)dy$ measures a different deficit. Both have dimensions of length, while their ratio $H = \delta^*/\theta$ characterises profile shape. Neither thickness is defined by a particular percentage edge speed.

Integrating the streamwise boundary-layer momentum equation and using continuity to eliminate the edge-normal flux yields

$$\frac{\tau_w}{\rho U_e^2} = \frac{d\theta}{dx} + (2 + H)\frac{\theta}{U_e}\frac{dU_e}{dx}.$$

The edge pressure gradient follows outer inviscid flow through $dp_e/dx = -\rho U_e\, dU_e/dx$. Under uniform outer speed the equation reduces to

$$d\theta/dx = C_f/2,$$

$$C_f = \tau_w/(\rho U_e^2/2).$$

With an adverse pressure gradient the second term is negative, and an increasingly thickening layer can still have very small or negative wall shear. Applying the uniform-speed relation outside its conditions would overestimate shear near separation.

Derive an approximate flat-plate law

Assume a laminar zero-pressure-gradient layer with $u/U = 2\eta - \eta^2$ for $0 < \eta = y/\delta < 1$ and outer speed beyond. The profile satisfies no slip at the wall, reaches the edge speed and has zero first derivative at its nominal outer edge. Integrating gives $\delta^* = \delta/3$, $\theta = 2\delta/15$, while the wall gradient gives

$$\tau_w = 2\mu U/\delta.$$

Substitute into the momentum integral and integrate from the leading edge:

$$\delta = \sqrt{\frac{30\nu x}{U}},$$

$$C_{f,x} = \frac{4}{\sqrt{30 Re_x}},$$

$$Re_x = \frac{U x}{\nu}.$$

The coefficient 0.730 from this approximate profile differs from the exact Blasius laminar result 0.664 while reproducing the square-root scaling. Profile choice closes an otherwise exact integrated balance and creates a measurable modelling error. It also treats the local leading-edge region outside its proper thin-layer asymptotics. Refining numerical integration of the same polynomial cannot eliminate the profile approximation.

For air with $U = 5.0$ m/s, $\nu = 1.5 \times 10^{-5}$ square metres per second, $x = 0.20$ m and $\rho = 1.2$ kg/m³, $Re_x = 6.67 \times 10^{4}$ and predicted $\delta = 4.24$ mm. The approximate local $C_f = 0.00283$ gives $\tau_w = 0.0424$ Pa. If a pressure-gradient or transition changes the profile appreciably, measure the actual shape and its x variation rather than applying this laminar estimate.

Compare the local velocity profile and wall stress with the boundary-layer chapter

Use a probe traverse to measure a momentum deficit

A small velocity probe is moved away from a smooth plate in increments of known height. Calibrate zero height and measure outer velocity independently. Convert the measured values to ratios with the outer velocity, integrate the displacement and momentum kernels using the same station coordinates, and repeat downstream. Even if the probe misses the point where the speed first reaches 99 percent of the outer value, the two integrals can remain informative. A contaminated outer-velocity estimate, however, leaves a persistent offset in the integrands across the entire outer part of the traverse.

Open the live experiment

Try the calculation

Outer speed (m/s) **5**

Kinematic viscosity (mm²/s) **15**

Plate station (m) **0.2**

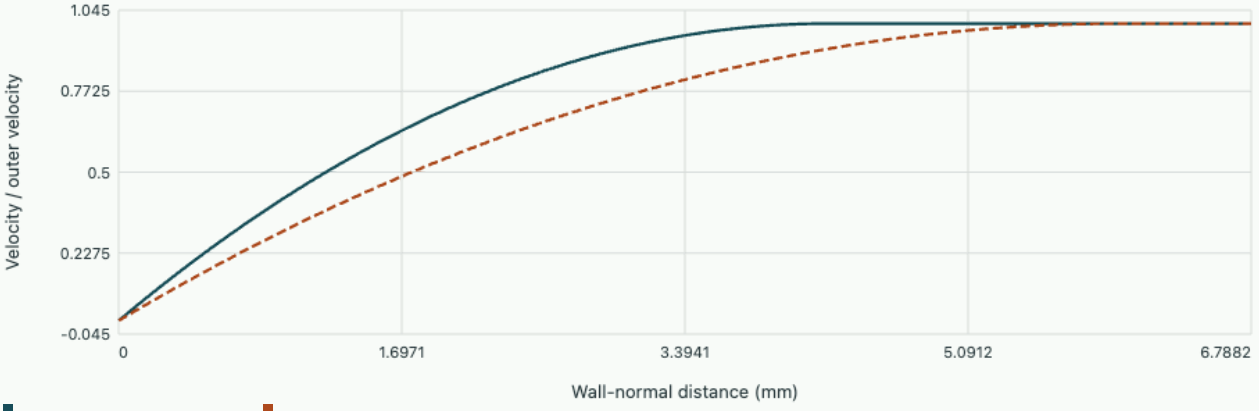

Selected station Twice the distance downstream

The quadratic trial layer has thickness 4.24 mm, displacement thickness 1.41 mm and local friction coefficient 0.00283. Smooth, laminar, zero-pressure-gradient conditions are assumed.

The model overlays a profile at a selected station and at twice that station distance. In a zero-pressure-gradient laminar layer both curves collapse if wall-normal position is divided by its own thickness. The outer velocity is the same in both plots and the wall slopes differ by a factor of the square root of two. This shows why a constant free-stream speed does not imply constant wall shear. Wall shear depends on the gradient normal to the wall, and diffusion spreads the velocity change over a progressively thicker layer.

For an independent check take a measured momentum thickness of 0.55 mm at a station and 0.66 mm at a station 60 mm downstream. Their finite difference gives a slope of 0.00183 and hence a mean skin-friction coefficient of 0.00367 under uniform outer speed. A measurement error of 0.02 mm at each station, treated as independent, corresponds to roughly one quarter of the measured difference. Improving one individual profile is not enough if the station separation is too small to resolve a change. Increasing separation improves signal but averages over more streamwise development. Repeating over several separation distances exposes that tradeoff and can reveal transition within the interval.

If the same probe is used at both stations, a common calibration gain can cancel in the normalised velocity ratios. An error in the zero wall distance affects the inner region differently. Repeat the integration after deliberately shifting the nominal wall location by its measured positioning uncertainty.

Tutorial · Infer drag from two traverse stations

A constant-speed incompressible layer has momentum thickness 0.30 mm at one station and 0.50 mm 0.15 m farther downstream. With $U = 5.0$ m/s and $\rho = 1.2$, estimate mean wall shear over the interval

and total drag on a strip of width 0.20 m.

▼ **Integrate the momentum relation**

Mean shear is

$$\rho U^2 \Delta\theta/\Delta x = 1.2(25)(0.00020)/0.15 = 0.040\,\mathrm{Pa}.$$

The area is 0.030 square metres, so drag is 1.20 mN. This estimate uses the complete momentum deficit and does not require differentiating a noisy near-wall velocity. It does require both profiles to cover the entire defect region and share a calibrated outer speed.

Tutorial · Check an apparent separation claim

At one location $H = 2.5, \theta = 1.0$ mm, $U_e = 4.0$ m/s, $dU_e/dx = -8.0$ per second and $d\theta/dx = 0.010$. Infer wall shear sign. Would the same momentum-thickness growth guarantee that sign in zero pressure gradient?

▼ **Retain the pressure-gradient term**

The dimensionless right side is $0.010 + 4.5(0.001/4)(-8) = 0.0010$, still positive but only one tenth of the zero-gradient estimate. In this example both cases have positive shear, yet a slightly stronger adverse gradient would reverse the indicated sign. Near zero the differences among several measured terms magnify relative uncertainty. A near-wall direction measurement or oil-film shear indicator can help distinguish a true sign reversal from fitted profile noise.

Tutorial · Detect a probe that misses the outer deficit

A traverse stops at the first point where measured speed reaches 97 percent of the apparent outer value. How might this bias displacement and momentum thickness, and how would you design a convergence check?

▼ **Integrate the remaining positive tail**

For an attached monotone profile both integrands are positive below the true outer speed, so prematurely truncating usually underestimates both thicknesses. Near the edge their integrands become similar because $u/U_e \simeq 1$; even a small speed defect over a broad tail can contribute appreciable area. Extend the traverse and compare integrals as the cutoff rises. Independently estimate true undisturbed U_e: a slight bias in that denominator can create a false nonzero tail over the entire outer integration region. Repeat at finer near-wall spacing too, separately testing quadrature and physical domain coverage.

MIT Aerodynamics of Viscous Fluids · boundary layers and momentum-integral methods

Momentum, motion and transport in fluids · 5. How long does a moving wall take to set a fluid layer in motion?

Start the top of a narrow gap suddenly and follow the velocity, volume flow and wall stresses as viscous diffusion builds a Couette profile.

Remove the final state before separating variables

Take two large, parallel plates separated by H, with $y = 0$ at the fixed plate. The liquid starts from rest. At $t = 0$ the upper plate begins to move at constant speed U. For an incompressible Newtonian liquid with no imposed pressure gradient, the unidirectional velocity $u(y, t)$ has zero convective acceleration. The streamwise momentum balance on a thin slice then reduces to

$$\rho\, \partial_t u = \partial_y(\mu\, \partial_y u).$$

With constant viscosity, kinematic viscosity $\nu = \mu/\rho$ is the momentum diffusivity.

Use $\eta = y/H$ and $F = \nu t/H^2$. The linear profile $u/U = \eta$ solves the eventual steady equation and both wall conditions. Subtract it by setting $w = u/U - \eta$. Both boundaries now require $w = 0$, which selects eigenfunctions $\sin(n\pi\eta)$ for $w_F = w_{\eta\eta}$. Each amplitude decays as $\exp(-n^2\pi^2 F)$. The interior initially has $w = -\eta$. Multiplying by a sine and integrating from zero to one gives

$$b_n = -2\int_0^1 \eta \sin(n\pi\eta)\, d\eta = 2(-1)^n/(n\pi).$$

Combining the parts gives

$$\frac{u}{U} = \eta + \frac{2}{\pi}\sum_{n=1}^{\infty} \frac{(-1)^n}{n} \sin(n\pi\eta) e^{-n^2\pi^2 F}.$$

For any positive time, higher modes decay rapidly. At the initial top corner the sudden change in surface velocity conflicts with the initially resting liquid. The mathematical wall gradient there diverges as $t \downarrow 0$. A finite starting acceleration would regularize that prediction. Fluid well away from that wall sees little change until the diffusion distance, of order $\sqrt{\nu t}$, becomes comparable with its distance to the moving surface.

Distinguish stored momentum from transmitted shear

Integrating the profile over the gap eliminates the even sine modes. The dimensionless volume flow per unit span becomes

$$q/(UH) = 1/2 - (4/\pi^2) \sum_{n\ \text{odd}} e^{-n^2\pi^2 F}/n^2.$$

Differentiating at the walls gives

$$\tau_{\mathrm{top}}/(\mu U/H) = 1 + 2\sum_{n} e^{-n^2\pi^2 F},$$

$$\tau_{\mathrm{bottom}}/(\mu U/H) = 1 + 2\sum_{n} (-1)^n e^{-n^2\pi^2 F}.$$

Here both symbols report μu_y evaluated in the positive y direction. The forces on the fluid act in opposite directions, so the net streamwise force per unit plate area is $\tau_{\mathrm{top}} - \tau_{\mathrm{bottom}}$.

Set $H = 4$ mm, $\nu = 1.6 \times 10^{-5}$ m^2/s, $\rho = 900$ kg/m^3 and $U = 0.20$ m/s. The gap diffusion time is 1 s. At 0.1 s the flow is $0.34894UH$, already 69.8% of its final value. The wall gradients still differ sharply, measuring 1.7843 and 0.2929 times the eventual shear of 0.72 Pa. Integrating the original momentum equation over the layer verifies that their difference accelerates the stored streamwise momentum, $\rho\, dq/dt$.

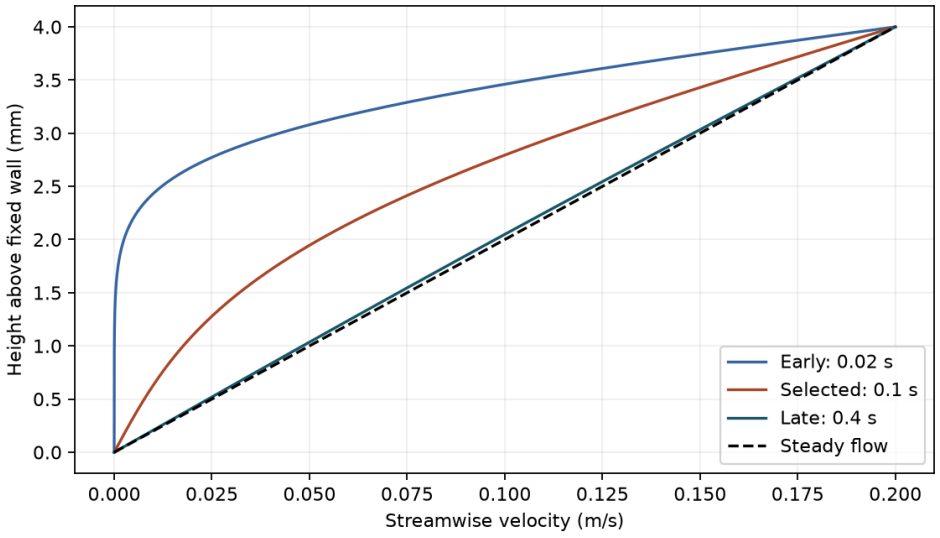

The top wall fixes the velocity at one end immediately. The curvature in the interior tracks how momentum is still entering the liquid.

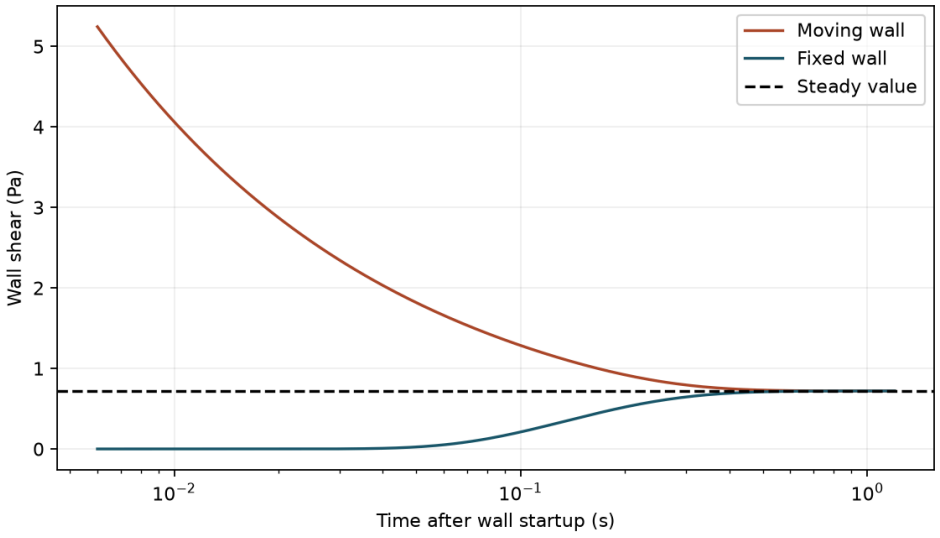

Initially the driving wall accelerates the upper layer. The fixed wall feels an appreciable force later, even as the force required at the driving wall declines.

Problem 1 · Predict the flow-settling time

Estimate when the flow reaches 99% of its final value. Why is one mode enough for this estimate?

▼ **Work through the solution**

Divide the missing flow by its final value to obtain $(8/\pi^2)\sum_{n\ \mathrm{odd}} e^{-n^2\pi^2 F}/n^2$. Its leading term reaches 0.01 at $F = \ln[8/(0.01\pi^2)]/\pi^2 = 0.44532$, or 0.44532 s with the given gap. At this time the next contributing mode contains $e^{-9\pi^2 F}/9$, below 10^{-17}. At much earlier times several modes reconstruct the thin moving layer.

Problem 2 · Double the gap

The plate speed and liquid stay fixed while H doubles. Compare the 99% settling time, steady shear, and steady flow per unit width in the two gaps.

▼ **Work through the solution**

The dimensionless solution reaches the same settling criterion at the same F. Since $t = FH^2/\nu$, the wider gap takes four times as long, about 1.78 s. The steady gradient is U/H, so its shear halves to 0.36 Pa. The steady flow is the area under a triangle of height U and width H, namely $UH/2$. It doubles to 8.0×10^{-4} m^2/s.

Interactive calculation · Startup couette

Change the physical and numerical inputs of the notebook model. Compare the updated curves and balance checks with the recorded notebook figures. Each plot uses the same equations and assumptions documented in that notebook; its readout names any analytical or reduced-model reference.

Open this live calculation

Try the calculation

Wall gap (mm)	**4**
Wall speed (m/s)	**0.2**
Fourier time νt/h²	**0.1**

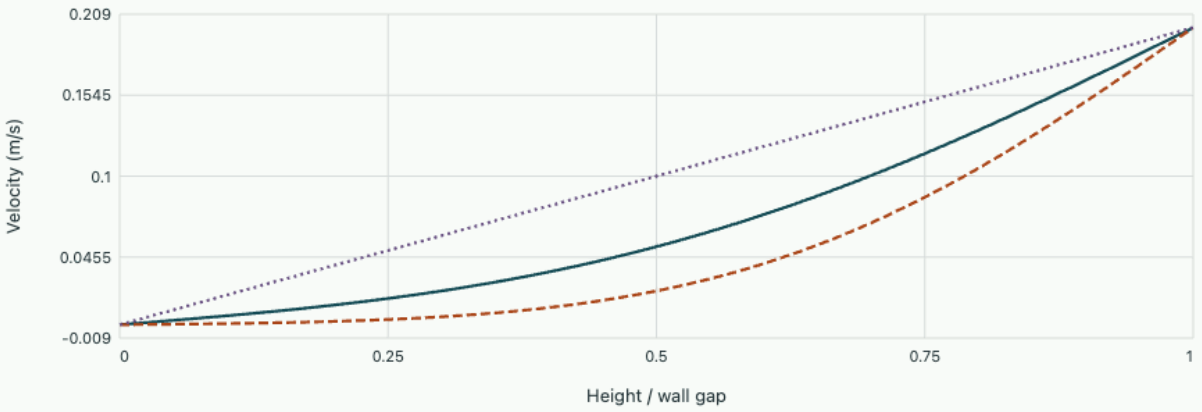

Selected time | Earlier, half Fourier time | Steady Couette profile

For ν=1.6×10⁻⁵ m²/s, selected time 0.100 s. The100-mode series satisfies no-slip at both walls; startup is instantaneous.

Download this example's editable notebook

Interactive calculation · Startup shear

Change the physical and numerical inputs of the notebook model. Compare the updated curves and balance checks with the recorded notebook figures. Each plot uses the same equations and assumptions documented in that notebook; its readout names any analytical or reduced-model reference.

Open this live calculation

Try the calculation

Wall gap (mm)	4
Wall speed (m/s)	0.2
Kinematic viscosity (mm²/s)	16

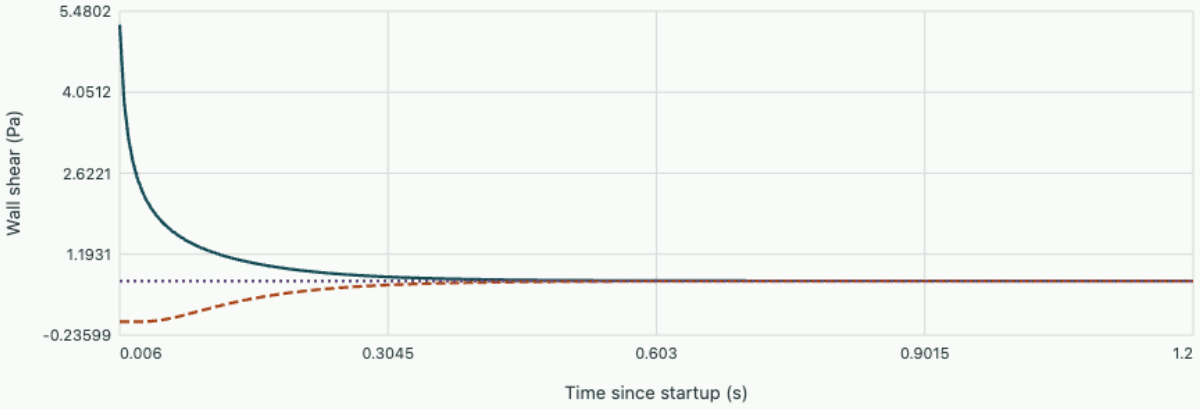

Diffusion time 1.000 s; steady shear 0.720 Pa at density900 kg/m³. The initial moving-wall stress is singular, so the plotted range starts at finite time.

Download this example's editable notebook

Open editable notebook Download .ipynb

Momentum, motion and transport in fluids · 6. How far upstream does a downstream water level matter?

A depth gauge downstream of a change in bed level measures a local state. Predict the depth one kilometre upstream by combining energy, cross-section geometry and a resistance law, then fit the roughness against independent uniform-flow readings.

Separate normal depth and critical depth

Consider steady flow at discharge Q in a long prismatic rectangular channel of width b. Depth y sets area $A = by$, wetted perimeter $P = b + 2y$ and hydraulic radius $R = A/P$. For a long reach of uniform depth, weight down the slope balances wall shear over the wetted perimeter. If $S_0 = -dz_b/dx$ is the bed slope, the force balance gives $\tau_0 = \rho g R S_0$. A resistance relation from measurement closes this balance. In SI units the Manning convention is

$$Q = \frac{1}{n} A R^{2/3} \sqrt{S_f},$$

$$S_f = \left(\frac{nQ}{AR^{2/3}} \right)^2.$$

Normal depth y_n solves $S_f = S_0$. Roughness n has units s m$^{-1/3}$. The equivalent Chézy form $U = C\sqrt{RS_f}$ has $C = R^{1/6}/n$ for the same prediction. Critical depth follows from specific energy $E = y + Q^2/(2gA^2)$ at fixed discharge. Differentiating gives $1 - Q^2 b/(gA^3) = 0$ at y_c. The critical condition contains no roughness. For $b = 4$ m, $Q = 6$ m³/s, $S_0 = 0.001$ and $n = 0.030$, $y_n = 1.556$ m while $y_c = 0.612$ m. This bed is mild for the specified discharge.

Derive an evolution equation in space

Assume hydrostatic pressure, negligible local losses, unit velocity-energy coefficient and a sufficiently gentle surface slope. Along increasing downstream distance the energy head drops by S_f per metre. Differentiating $H = z_b + y + Q^2/(2gA^2)$ and using $dA/dy = b$ gives

$$\frac{dy}{dx} = \frac{S_0 - S_f(y)}{1 - Fr^2(y)},$$

$$Fr^2 = \frac{Q^2 b}{gA^3}.$$

A downstream weir may impose a subcritical stage. For $y > y_n > y_c$ we have $S_f < S_0$ and $Fr < 1$, so $dy/dx > 0$. The water is deeper toward the control and approaches normal depth upstream. Integrate toward decreasing x starting at the measured stage. Replacing R by y assumes a very wide channel, which the 4 m section does not justify at these depths. Close to $Fr = 1$ the denominator signals the limit of a smooth slowly varying profile. A jump requires its own momentum treatment.

Separate resistance calibration from the boundary condition

The notebook first fits one roughness to four synthetic uniform discharge measurements and then holds it fixed for two downstream controls. The fitted $n = 0.03001$ gives depths of 1.605 m and 1.745 m one kilometre upstream of outlet depths of 1.8 and 2.2 m. The downstream 0.4 m difference has decayed substantially and still leaves an observable upstream effect.

Interactive experiment · Change a downstream control and recompute its upstream reach

The live calculation integrates the depth equation upstream with fourth-order Runge–Kutta steps of 2 m. Keep the default discharge and roughness, move the outlet stage from 1.8 to 2.2 m and compare depths 1 km upstream. Next change roughness: normal depth moves, while critical depth stays fixed. Changing discharge moves both reference depths.

The channel remains 4 m wide with bed slope 0.001. All available input combinations stay subcritical, where a downstream stage can influence the upstream reach. The plotted coordinate increases upstream, so its derivative has the opposite sign to the downstream equation. The notebook below fits roughness with OneSimulation before integrating two profiles; the browser lets you explore the consequences of prescribing that coefficient directly.

Open this experiment online

Try the calculation

Discharge (m³/s)	6
Manning roughness (s/m⅓)	0.03
Outlet depth (m)	2.2

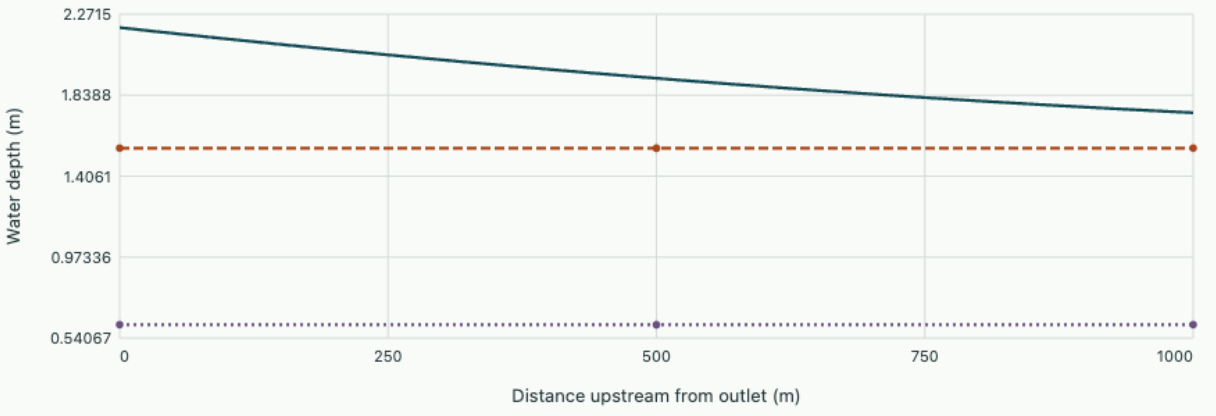

At 1 km upstream: 1.745 m. Normal depth 1.556 m; critical depth 0.612 m. Outlet Froude number 0.147. Fixed 4 m width and 0.001 bed slope; upstream RK4 steps are 2 m. The selected range stays subcritical.

Continue in the OneSimulation notebook · Download its Python model

OneSimulation experiment · Two downstream stages produce different upstream profiles at the same calibrated roughness

Run the notebook with OneSimulation 0.2.0, NumPy, SciPy and Matplotlib. Change the input data and compare your run with the recorded result.

```
"""Infer Manning roughness from uniform flow, then predict a subcritical backwater."""
import numpy as np
import matplotlib.pyplot as plt
from scipy.integrate import solve_ivp
from onesim.numerics.nonlinear import LeastSquares

width, slope, discharge, gravity = 4.0, 0.001, 6.0, 9.81
measured_depth = np.array([0.7,0.85,1.0,1.15])  # m
def section(depth):
    area = width*depth
    return area, area/(width+2*depth)
def uniform(depth, roughness):
    area, radius = section(depth)
    return area*radius**(2/3)*np.sqrt(slope)/roughness
measured_flow = uniform(measured_depth,0.030) + np.array([0.02,-0.03,0.02,-0.01])
fit = LeastSquares().solve(lambda n: uniform(measured_depth,n[0])-measured_flow,
                           [0.025], bounds=([0.010],[0.08]))
roughness = fit.x[0]
def depth_gradient(x, y):
    area,radius = section(y)
    friction = (roughness*discharge/(area*radius**(2/3)))**2
    froude_squared = discharge**2*width/(gravity*area**3)
    return (slope-friction)/(1-froude_squared)

fig, ax = plt.subplots(figsize=(6.4,3.7), layout="constrained")
print(f"fitted Manning n = {roughness:.5f} s/m^(1/3)")
for boundary in [1.8, 2.2]:
    x = np.linspace(0,-1000,250)
    sol = solve_ivp(depth_gradient,[0,-1000],[boundary],t_eval=x,rtol=1e-9,atol=1e-10)
    assert sol.success
    print(f"outlet {boundary:.1f} m: depth 1 km upstream = {sol.y[0,-1]:.3f} m")
    ax.plot(-sol.t,sol.y[0],label=f"Outlet depth {boundary:.1f} m")
ax.set(xlabel="Distance upstream from control (m)",ylabel="Flow depth (m)")
ax.legend()
plt.show()
```

Reference run

```
fitted Manning n = 0.03001 s/m^(1/3)
outlet 1.8 m: depth 1 km upstream = 1.605 m
outlet 2.2 m: depth 1 km upstream = 1.745 m
```

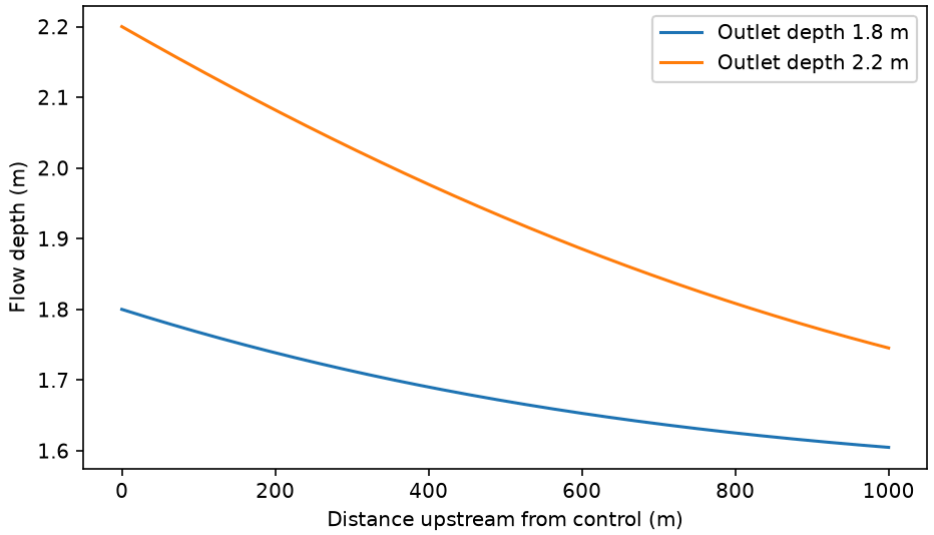

Two downstream stages produce different upstream profiles at the same calibrated roughness

Download editable notebook · Download Python script

Why two depth measurements do not always identify roughness

Near normal depth, the water surface changes slowly. Bed-slope bias, discharge error and roughness can produce similar residuals over a short reach. Calibrating against uniform measurements at more than one discharge gives an independent constraint before fitting the backwater.

Exercises on hydraulic controls

Two channels have the same discharge and width. Only the Manning coefficient is changed. Which characteristic depth changes?

▼ **Worked solution**

Critical depth is fixed by discharge and geometry. Increasing roughness lowers discharge capacity at fixed depth and slope, so normal depth must increase to carry the same discharge. An altered resistance can move the flow into a different profile class.

A subcritical section has $y = 2.0$ m in the example. Estimate the slope before integrating.

▼ **Worked solution**

Here $A = 8$ m², $R = 1$ m, $S_f = (0.03 \times 6/8)^2 = 0.0005063$ and $Fr^2 = 36(4)/(9.81 \times 512) = 0.0287$. Thus $dy/dx = 0.000508$ m/m. Extrapolating this local slope for a kilometre ignores its variation with depth.

Further reading · Gerhart, Hochstein and Gerhart, Munson, Young and Okiishi’s Fundamentals of Fluid Mechanics, 9th ed., Sections 10.3–10.6.

Momentum, motion and transport in fluids · 7. How can a constant-area duct choke?

A nozzle reaches a sonic state by changing area. A straight pipe can approach the same Mach number through friction or through heating. The two cases conserve different combinations of stagnation properties.

Choose the wall process before eliminating variables

Take a steady one-dimensional calorically perfect gas with $G = \rho u$ constant, no shaft work and constant pipe area. Write $M = u/\sqrt{\gamma RT}$, $h_0 = c_pT + u^2/2 = c_pT_0$. An adiabatic wall fixes T_0 even when wall friction creates entropy. A frictionless wall which supplies heat changes T_0 while preserving the axial momentum flux $p + \rho u^2$. Measure static and stagnation variables independently to distinguish these processes.

Integrate the frictional momentum loss

For hydraulic diameter D define the Darcy factor by $\tau_w = f_D\rho u^2/8$. A slice has perimeter-to-area ratio $4/D$, so momentum balance is $dp + \rho u\,du + f_D\rho u^2 dx/(2D) = 0$. Differentiate constant G and T_0 to obtain $d\rho/\rho = -du/u$ and $dT/T = -(\gamma-1)M^2 du/u$. Substitute in $dp/p = d\rho/\rho + dT/T$ and $dM/M = du/u - dT/(2T)$:

$$\frac{f_D dx}{D} = \frac{4(1-M^2)}{\gamma M^3[2+(\gamma-1)M^2]}\,dM.$$

Integrate from inlet M_1 to outlet M_2. Defining the remaining distance to sonic conditions by $F(1) = 0$ gives

$$\frac{f_D L}{D} = F(M_1) - F(M_2),$$

$$F(M) = \frac{1-M^2}{\gamma M^2} + \frac{\gamma+1}{2\gamma}\ln\frac{(\gamma+1)M^2}{2+(\gamma-1)M^2}.$$

For air with $\gamma = 1.4$, $M_1 = 0.4$, $M_2 = 0.7$, the two function values are 2.30849 and 0.20814. With $D = 0.050$ m and constant $f_D = 0.020$, the required length is 5.25 m. The maximum length at the stated inlet condition is 5.77 m. A longer duct requires different inlet conditions or mass flow. A quoted Fanning coefficient is one quarter of this Darcy coefficient.

Remove friction and allow heat transfer

The constant momentum flux becomes $p(1+\gamma M^2) = p^*(1+\gamma)$, where the star denotes the sonic state on this same momentum line. Use mass conservation and the ideal-gas law to get $T/T^* = [(1+\gamma)M/(1+\gamma M^2)]^2$. Multiply by the ratio between stagnation and static temperatures at each state to obtain

$$\frac{T_0}{T_0^*} = \frac{2(1+\gamma)M^2[1+(\gamma-1)M^2/2]}{(1+\gamma M^2)^2}.$$

For the same inlet and outlet Mach numbers this ratio rises from 0.52903 to 0.90850. If $T_{01} = 350$ K, the outlet stagnation temperature is 601.1 K. The heat added per unit mass for $c_p = 1005$ J/(kg K) is approximately 252 kJ/kg. The sonic-line maximum $T_0^* = 661.6$ K places an upper bound on additional heat at the fixed inlet state. In the friction case the stagnation temperature remained at 350 K throughout.

Why both subsonic cases accelerate

Mass flux per area is fixed. The change of pressure and temperature required by momentum and wall conditions reduces density on these subsonic paths. Velocity rises. Supersonic and subsonic branches require explicit tracking when inverting a sonic-reference relation.

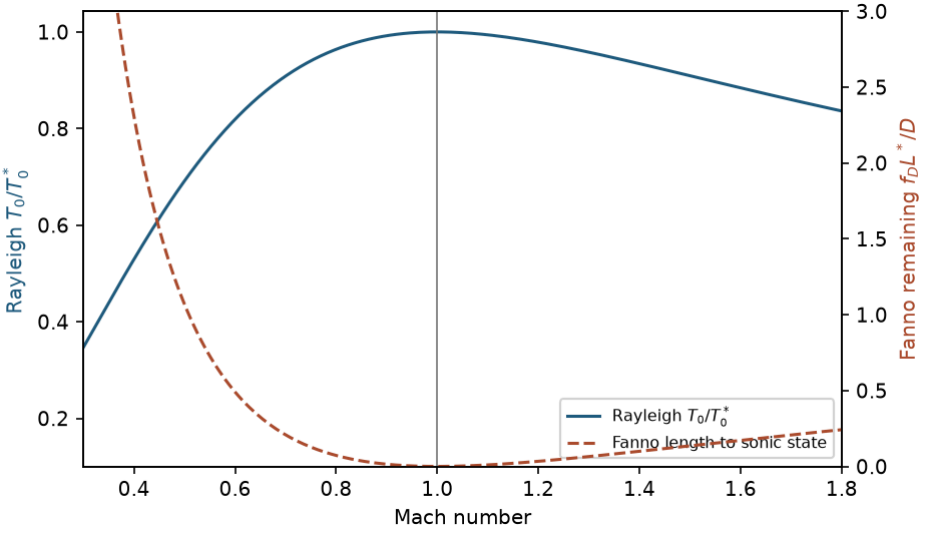

Separate wall-process models plotted at the same Mach number. The blue Rayleigh curve uses the left axis, the dashed Fanno curve the right axis. Both have a sonic reference at Mach one.

Interactive calculation · Approach a sonic state by two different wall processes

Vary the heat-capacity ratio and inlet Mach number. Compare the remaining friction-length budget with the heat addition required to reach the Rayleigh sonic reference. The two dimensionless ordinates have different definitions.

Open this live calculation

Try the calculation

Heat-capacity ratio **1.4**

Inlet Mach number **0.6**

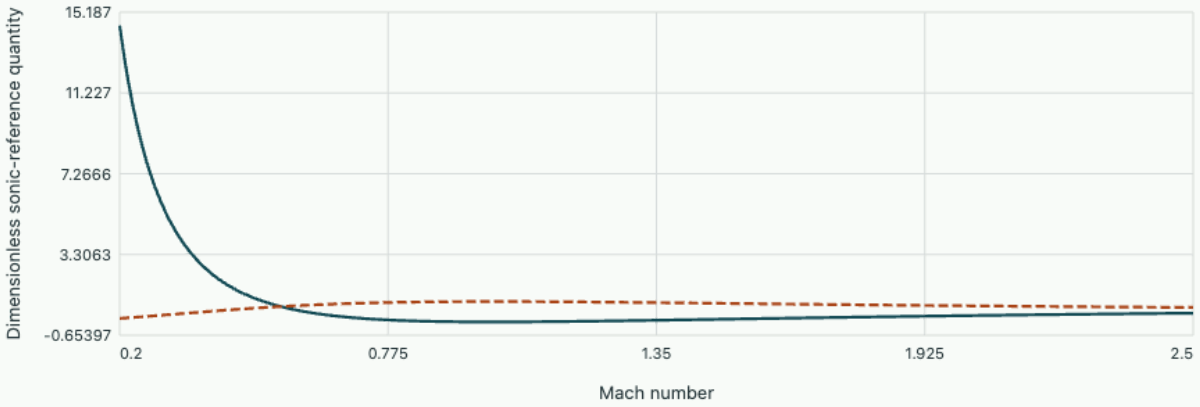

From inlet Mach 0.600, Fanno remaining fD L/D=0.491; Rayleigh heat addition to choke is 0.221 times inlet cp T0. The curves describe two different wall processes and use independent dimensionless quantities.

Exercises on distinguishing mechanisms

A frictional pipe with the worked inlet already carries gas at Mach 0.7 at a pressure tap. How much more straight pipe reaches the mathematical choking limit?

▼ **Worked solution**

The remaining friction length is $DF(0.7)/f_D = 0.520$ m. This calculation assumes the same Darcy factor up to the sonic state.

A well-insulated pipe test gives a large stagnation-pressure loss but nearly identical measured stagnation temperatures. Could a frictionless Rayleigh model with steady net heating explain both

quantities?

▼ **Worked solution**

Net heating necessarily raises h_0. The nearly unchanged stagnation temperature supports adiabatic frictional loss or another adiabatic irreversible process. Static temperatures alone do not distinguish acceleration from wall heat.

Further reading · Gerhart, Hochstein and Gerhart, Munson, Young and Okiishi's Fundamentals of Fluid Mechanics, 9th ed., Sections 11.8–11.9.